JOURNAL OF Materials CHEMISTRY

Influence of surface reactions and ionization gradients on junction properties of $F_{16}PcZn$

Stefan Hiller,[a] Derck Schlettwein,*[b,c] Neal R. Armstrong[c] and Dieter Wöhrle*[a]

[a]*Institut für Organische und Makromolekulare Chemie, Universität Bremen, Fachbereich 2 (Biologie, Chemie), Postfach 330 440, 28334 Bremen, Germany*

[b]*Institut für Angewandte und Physikalische Chemie, Universität Bremen, Fachbereich 2 (Biologie, Chemie), Postfach 330 440, 28334 Bremen, Germany*

[c]*Department of Chemistry, University of Arizona, Tucson, AZ 85721, USA*

Compared to unsubstituted phthalocyaninatozinc(II) (PcZn), electron withdrawing fluorine atoms in hexadecafluorophthalocyaninatozinc(II) ($F_{16}PcZn$) cause a stabilization of the frontier orbitals of about 1.6 eV. This is concluded from photoelectron spectroscopy (UPS) at thin films on Au surfaces. From experiments at thin films [physical vapor deposition (PVD)] of PcZn deposited on top of $F_{16}PcZn$ under UHV conditions it is seen that a closed film of PcZn is formed at least within 5 nm average film thickness, that thermodynamic equilibrium between the films is achieved by charge transfer in redox reactions at the interface which, however, do not lead to a macroscopic space-charge layer. To study electrical device properties thin films of $F_{16}PcZn$ and PcZn were prepared in a range between 90 nm and 240 nm. Changes in electrical properties of ITO, Au|$F_{16}PcZn$|metal (metal = In, Au) and ITO|$F_{16}PcZn$|PcZn|Au devices have been studied in the dark and under illumination. Results of current–voltage characteristics and short-circuit photocurrent spectra of devices as prepared and measured under high vacuum (HV, 10^{-5}–10^{-6} mbar) and after exposure to air are presented. In vacuum symmetrical $I(U)$ characteristics were found for ITO|$F_{16}PcZn$|Au devices. After exposure to air a decrease in dark conductivity, unsymmetrical $I(U)$ characteristics and a considerable photovoltage (U_{OC}) was measured under illumination. The magnitude of U_{OC} as well as its direction can be clearly correlated with the exposure to atmosphere. This observation leads to a discussion based on a local asymmetry in O_2 content as caused by slow diffusion into $F_{16}PcZn$. O_2 would lead to a decrease in the local majority carrier density as typically expected for organic n-type conductors. Rectification found in $F_{16}PcZn$|In devices can be explained by a chemical reaction between the distinct electron acceptor $F_{16}PcZn$ and In as a donor. Photocurrent action spectra of devices with different thicknesses of $F_{16}PcZn$ layers in ITO|$F_{16}PcZn$|PcZn|Au revealed detailed information about the site of charge carrier generation (photoactive area). The junction properties are discussed in detail based on the frontier orbital positions of PcZn and $F_{16}PcZn$, and the work functions of the corresponding electrode materials.

Introduction

Thin films of phthalocyaninatozinc(II) (PcZn) exhibit p-type behavior due to the doping with electron accepting molecular oxygen.[1] Results of conductivity and Seebeck measurements reveal that after interaction with O_2, PcZn belongs to the group of narrow band semiconductors involving charge carrier transport rather well described in terms of the band model.[2] High thermal stability, simple synthesis and high absorption coefficients for visible light are features of this material, and of phthalocyanines (Pcs) in general. These properties resulted in a number of studies aiming at different applications like photovoltaic cells,[3–5] rectifying junctions[6] and gas sensors.[7] Pcs are already successfully marketed as charge-generating layers in electrophotography[8] due to their high photoconductivity which quickly relaxes to the dark value.

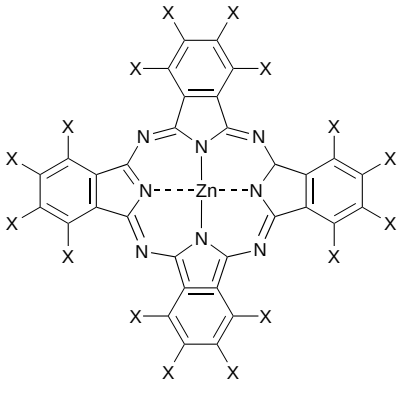

$F_{16}PcZn$: X = F
PcZn : X = H

Chemical modification of Pc ligand has proven to be a powerful tool for tailoring the electronic properties of the molecule and thereby the electrical properties of the solid.[9–12] For the electrical characterization of pure molecular materials, physical vapor deposition (PVD) has turned out to be the most successful film preparation technique as it allows reproducible preparation of pure films and, as it is a vacuum technique, it excludes uncontrolled influences of the ambient. The number of Pcs with electronically relevant chemical substituents, which are suitable for PVD however, is rather limited due to thermal instability. Tetrapyridotetraazaporphyrinatozinc(II) (TPyTAPZn), for example, has been characterized as a molecular n-type semiconductor by photoelectrochemical, conductivity and thermopower experiments.[2,12–14] The electronic conductivity is caused by redox interactions with donor levels even under UHV conditions with the electronic system of TPyTAPZn which is stabilized by about 0.4 eV relative to PcZn as revealed by UPS and VIS spectroscopy studies.[10,15]

We investigated PVD compatible phthalocyanines fluorinated at the ligand as another approach to reach n-type behavior. Recently rectification in Au|PcNi|F_8PcCu|Au devices was observed.[6,16] This behavior was explained by the formation of a pp′-isotype heterojunction based on band tuning *via* ring peripheral electron withdrawing fluorine groups. The perfluorinated 1,2,3,4,8,9,10,11,15,16,17,18,22,23,24,25-hexadecafluorophthalocyaninatozinc(II) ($F_{16}PcZn$) has also been synthesized and studied for applications in photodynamic cancer therapy[17] and an electrocatalyst for the reduction of dioxygen.[18] In earlier studies we established n-type conductivity for $F_{16}PcZn$[13,14] again caused by stabilization of the frontier orbitals by the strongly electron-withdrawing F atoms.[15,19] In

the present contribution our interest is focused on the characterization of F_{16}PcZn thin films in contact with metals with different work functions and with PcZn, both in vacuum and after exposure to air. Current–voltage plots and short circuit photocurrent spectra combined with UPS of the junction enable us to discuss in detail the site of photocarrier generation as well as the junction properties. Open circuit voltage measurements over a long period of time after first exposure to air were carried out to demonstrate the strong influence of oxygen as acceptor. The combination with conductivity measurements leads to a detailed discussion about the different effects of ambient atmosphere.

Experimental

F_{16}PcZn was synthesized by heating a 4:1 mixture of sublimed 3,4,5,6-tetrafluorophthalo-1,2-dinitrile and zinc acetate dihydrate in a vacuum-sealed glass tube for 1 h at 180 °C. The resulting dark blue powder was treated in a Soxhlet apparatus with water and light petroleum (bp 100–120 °C) to remove inorganic and organic contaminants. PcZn was commercially available from Aldrich (Germany). Both materials were purified by sublimation in a three-zone oven (Lindberg, Watertown USA) *in vacuo* (10^{-5} mbar) at 420 °C for F_{16}PcZn and at 400 °C for PcZn. Each sublimation was performed once as this had proven to be sufficient in a study of photovoltaic properties of PcZn in an earlier study where repeated sublimations led to no significant change.[4] F_{16}PcZn was characterized by DCI mass spectrometry and VIS spectroscopy. The VIS spectra were in good agreement with the literature.[20] Aside from the molecular ion peak of F_{16}PcZn at $m/z = 864$ with the correct isotopic distribution pattern, small amounts of F_{15}HPcZn ($m/z = 846$) of less than about 2% and of 3,4,5,6-tetrafluorophthalo-1,2-dinitrile ($m/z = 200$) were detected in the mass spectra. The temperature dependence of the MS signals revealed similar sublimation temperatures for F_{16}PcZn and F_{15}HPcZn which did not allow their separation by sublimation. The dinitrile was detected only at higher evaporation temperatures indicating that it originated from decomposition of F_{16}PcZn at higher evaporation temperatures. The sublimation was therefore performed at the minimum possible temperature of 420 °C.

Ultraviolet photoelectron spectroscopy (UPS) was performed on thin films deposited on atomically clean (Ar cation bombardment, analyzed by Al-Kα XPS) polycrystalline Au surfaces (99.99%, Aldrich) by use of the HeIα line (21.2 eV) from a capillary discharge lamp in a VG Escalab MKII spectrometer at a constant retard ratio of 4. F_{16}PcZn and PcZn were vapor-deposited from BN crucibles (R. D. Mathis) in a UHV chamber (base pressure 10^{-8} mbar) which was connected to the spectrometer. The temperature of the crucible was measured using a chromel–alumel thermocouple and controlled (Omega CN-310) by resistive heating through a Ta wire. After degassing at lower temperatures (*ca.* 100 °C) the temperature was slowly altered until a deposition rate of typically 0.1 nm min^{-1} was achieved. The rate and the deposited amount were measured by shifts in the resonance frequency of a quartz crystal (10 MHz, ITT 2485) mounted 10 mm from the substrate. Spectra were collected in vacuum by transfer of the sample into the analyzer chamber. This sequence was repeated until the features in the spectra arising from the sample material could be clearly analyzed and a sufficiently constant energy of the HOMO, as referred to the energy of an electron in vacuum, was obtained. As a reference the onset of emission at lowest kinetic energy (binding energy + work function = energy *vs.* vacuum = 21.2 eV) was used which was detected after applying a bias voltage of 5 V.[15] A sum of Gaussian signals was assumed and fitted to the data in order to determine the position of each emission band.

Photoelectrical measurements were performed on a glass substrate coated with semitransparent ITO (indium tin oxide) with an average thickness of 20 nm and a surface resistance of 200 Ω □$^{-1}$ commercially available from Flachglas Ag (Germany). The total size of the glass substrate was 25 mm × 50 mm etched with a paste of zinc powder and water dipped into concentrated HCl for a few seconds leaving an area covered by ITO of 15 mm × 50 mm. Subsequently the substrates were successively treated in an ultrasonic bath with acetone, distilled water, distilled water with detergent and *tert*-butyl alcohol for at least 10 min each (all solvents of analytical grade). Precleaned substrates were stored under *tert*-butyl alcohol. Gold and indium were purchased in coating quality (99.99%, Balzers). A variable mask system was used during sublimation to obtain single- and double-layer cells. In a first step one or two organic dyes were sublimed in a high vacuum system (CJT, Germany) one after the other onto the substrate from alumina crucibles at pressures in the range 10^{-6}–10^{-5} mbar. The source–substrate distance was about 25 cm and the source–source distance was about 10 cm. Due to the distance between source and substrate the average substrate temperature was below 40 °C during deposition. Film thickness was monitored by an oscillating quartz crystal (Martek TM100) and examined by Slown Dektak IIA measurements. Typical material densities are 2.03 g cm^{-3} (F_{16}PcZn), 1.9 g cm^{-3} (PcZn), 19.3 g cm^{-3} (Au) and 7.31 g cm^{-3} (In). The organic film thickness of double layer and single layer devices was varied between 90 and 250 nm. Gold and indium top electrodes up to 50 nm and 150 nm were used. Sublimation rates were in the ranges 12–18 nm min^{-1} (organics and In) and 3–6 nm min^{-1} (Au). The active area of each cell varied between 0.09 cm^2 and 0.18 cm^2. Samples for solid state VIS absorption spectra were prepared the same way on fused silica.

A voltage scan generator (Bank VSG83, Germany) in combination with an Electrometer (Keithley 610 C) was used to obtain current–voltage plots. All data were recorded digitally by a Keithley DMM 2000 connected to a personal computer system. The polarity of all potentials is given for the ITO electrode. The light source used for white light illumination (100 mW cm^{-2}) was a 1000 W xenon arc lamp (LOT Oriel). Monochromatic illumination for short circuit photocurrent spectra with constant 10^{15} photons s^{-1} cm^{-2} through ITO and 10^{14} photons s^{-1} cm^{-2} through gold over the total spectral range was obtained by use of interference filters (LOT Oriel) with a half height of 10 nm. Light intensities were measured with a calibrated photodiode (BPX/65). Measurements were exclusively made after about 2 h under HV to allow thermal relaxation.

Results

(a) VIS spectroscopy

Fig. 1(a) shows the VIS spectra of PcZn (dotted line) and F_{16}PcZn (straight line) in 1-chloronaphthalene at room temperature. Absorption maxima for the Q-band are seen at 678 nm with shoulders at 612 and 648 nm for PcZn, and at 686 nm for F_{16}PcZn with shoulders at 617 and 654 nm. The shoulders are typical for transitions into higher vibronic states of the excited state. The absence of any aggregation effects in both cases indicates monomer behavior in solution. The F_{16}PcZn Q-band is shifted in the bathocromic direction by 8 nm as compared to PcZn. This is expected from the inductive effect of the substituents.[21] In solid thin films on fused silica the Q-bands absorb in a much broader range. The bands shown in Fig. 1(b) are split into at least two bands in each case leading to two apparent maxima (612 nm and 698 nm for PcZn, 652 nm and 814 nm for F_{16}PcZn) typical for the interaction of adjacent molecules in organic crystals.[22–24] Optical absorption data can be used to estimate the frontier orbital gap of the investigated materials. If the energy of the Q-band

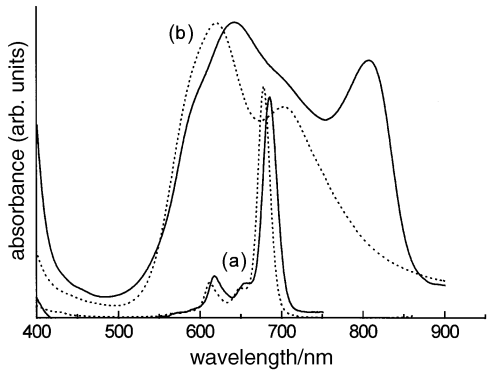

Fig. 1 Optical absorption spectra of F_{16}PcZn (—) and PcZn (– – –) dissolved in 1-chloronaphthalene (a) and as a solid film (75 nm) on a quartz substrate (b)

maximum at lowest energy is taken as the minimum value to create molecular excitons in the solid and if an exciton dissociation energy of 0.2 eV as determined from the activation energy of photoconductivity of PcZn[1,11] is assumed to be valid in both materials, HOMO–LUMO gaps of about 1.7 eV for F_{16}PcZn and 2 eV for PcZn are obtained.

(b) (ITO,Au)|PcZn|Au devices

As a prerequisite for the successful investigation of ITO|F_{16}PcZn|PcZn|Au junctions ITO|PcZn[150 nm]|Au and Au|PcZn[250 nm]|Au devices were characterized first. In the current–voltage characteristics symmetrical currents at positive and negative polarization ($r_{rf,\pm 0.25V}=1$) as well as a linear relationship of $I(U)$ was found up to ± 0.25 V (± 17 kV cm^{-1}) for films measured in vacuum demonstrating the ohmic contact behavior of PcZn to ITO and Au. The ohmic region was extended up to ± 1 V (± 67 kV cm^{-1}) in symmetrical Au|PcZn|Au junctions. The specific conductivity was calculated from eqn. (1) to be $\sigma_{301K,\pm 0.25V}=6\times 10^{-12}$ S cm^{-1} in Au|PcZn|Au and $\sigma_{301K,\pm 0.25V}=2\times 10^{-11}$ S cm^{-1} in ITO|PcZn|Au as prepared in vacuum.

$$\sigma = en\mu = \frac{I}{U}\frac{l}{q} \qquad (1)$$

where e is the charge of an electron, n the concentration of charge carriers, μ the mobility, I the observed current, U the applied voltage, l the film thickness and q the active area. Activation energies of $E_A=0.7$ eV for the conductivity of PcZn were estimated from the temperature dependence of Au|PcZn|Au devices (slope of a plot of log σ *vs.* $1/T$) in the range 321–433 K. Both results, σ and E_A, are in good agreement with the literature.[25,26] PcZn layers can be characterized as slightly p-doped insulators prepared in HV. Dark electrical properties are significantly changed during exposure to air. We measured a dark conductivity of up to $\sigma_{301K,0.25V}=3\times 10^{-7}$ S cm^{-1} for Au|PcZn|Au devices after 6 months in air. The strong increase of σ by more than four orders of magnitude at decreasing $E_A=0.3$ eV (251–303 K) is explained by the fact that electron accepting O_2 diffuses into the polycrystalline PcZn thin layers and leads to an increase of the total majority hole carrier concentration in a redox reaction reminiscent of doping in classical semiconductors. This was confirmed earlier by the positive Seebeck coefficient, S, of PcZn under pure oxygen atmosphere (200 mbar).[2] Comparison of the temperature dependences of S and σ shows that under these conditions charge transport in PcZn can be sufficiently interpreted in terms of a narrow band semiconductor.[2]

As expected for ohmic contacts, under illumination with white light no rectification was observed for ITO|PcZn|Au and Au|PcZn|Au in vacuum or after exposure to air. A small photovoltage U_{OC} of only a few mV with no preferred direction must be assigned to some defects in the contact areas.

(c) (ITO,Au)|F_{16}PcZn|Au devices

As prepared and measured under HV the $I(U)$ characteristics of ITO|F_{16}PcZn[150 nm]|Au [case 1 in Fig. 2] and Au|F_{16}PcZn[220 nm]|Au devices exhibit ohmic behavior in the dark in the region of ± 0.25 V ($r_{rf,\pm 0.25V}=1$) which corresponded to ± 16 kV cm^{-1} for the first and ± 11 kV cm^{-1} for the second device. The dotted line in Fig. 2 (inset) corresponds to a linear fit. Specific conductivities of $\sigma_{301K,\pm 0.25V}=2\times 10^{-10}$ S cm^{-1} (ITO|F_{16}PcZn[150 nm]|Au) and $\sigma_{301K,\pm 0.25V}=8\times 10^{-11}$ S cm^{-1} (Au|F_{16}PcZn[220 nm]|Au) were calculated. An activation energy of $E_A\approx 0.2$ eV in the range 300–363 K was determined from Arrhenius plots for both. As reported earlier, thermopower measurements on F_{16}PcZn thin films in vacuum revealed a negative sign for the Seebeck coefficient.[14] F_{16}PcZn is well described in terms of a weak n-type insulator. This example shows clearly that electron withdrawing ligands enable both frontier orbital tuning and change of the conduction type. This compound is generally much easier to reduce by charge donating molecules than the unsubstituted PcZn[15,19] which obviously leads to partial reduction by traces of donor molecules which are present even in HV but have not yet been identified. Consistently with the different conduction type, exposure to air for six months caused a significant decrease in conductivity to 3×10^{-12} S cm^{-1} (case 3 in Fig. 2). The presence of O_2 decreases the number of free majority carriers in combination with an increase in activation energy to $E_A\approx 0.4$ eV (299–367 K) over a period of six months.

In spite of the ohmic behavior in the dark a small U_{OC} value is reproducibly obtained under illumination which changes significantly in sign and magnitude during exposure to air. Fig. 3(a) depicts the dependence of the open circuit voltage on time for ITO|F_{16}PcZn|Au after first exposure to air over a period of up to several months. The first reading after 2 h in high vacuum (+7 mV) was obtained as prepared followed by readings after exposure to air at 37 days (−320 mV), 70 days (−490 mV), 160 days (−200 mV) and after one year (+5 mV). The devices were stored in the dark after each reading was taken. Although the changes in magnitude are significant the transient change in sign appears to be most characteristic. Devices stored under air for periods of about a year exhibited photovoltages close to those obtained under vacuum, but only after a period was finished of a rather high photovoltage in the opposite direction.

This result was confirmed by additional experiments on ITO|F_{16}PcZn devices stored in air for different periods before top electrode deposition [see Fig. 3(b)]. To obtain samples as

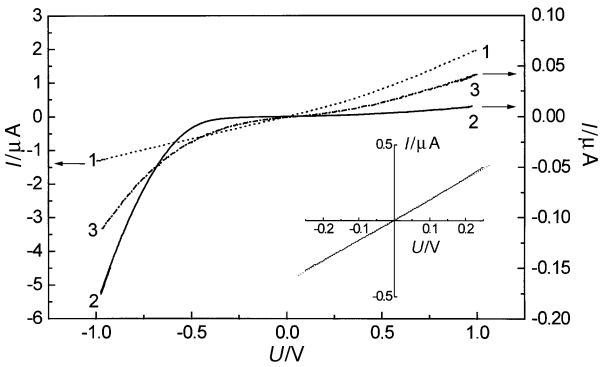

Fig. 2 Current–voltage characteristics for an ITO|-F_{16}PcZn[150 nm]|Au device over a range of ± 1 V in vacuum (– – –, 1) and under air for 880 (—, 2) and 4500 (–·–, 3) hours. Ohmic behavior in vacuum demonstrated by a linear current–voltage characteristic over a range of ± 0.25 V (inset, same sample).

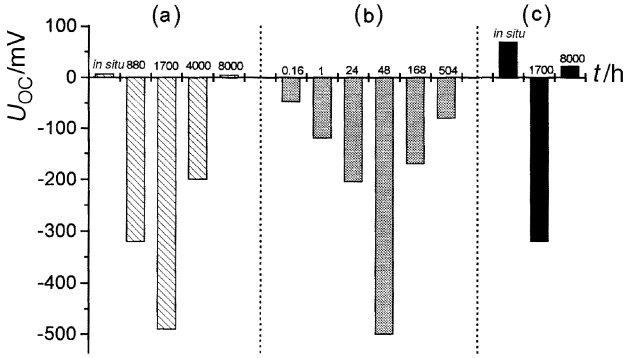

Fig. 3 Development of the open-circuit voltage over time for ITO|F_{16}PcZn[150 nm]|Au (a), ITO|F_{16}PcZn[240 nm],air|Au (b) and ITO|F_{16}PcZn[80 nm]|PcZn[80 nm]|Au (c) devices as prepared and after exposure to air. All samples were illuminated through the ITO electrode.

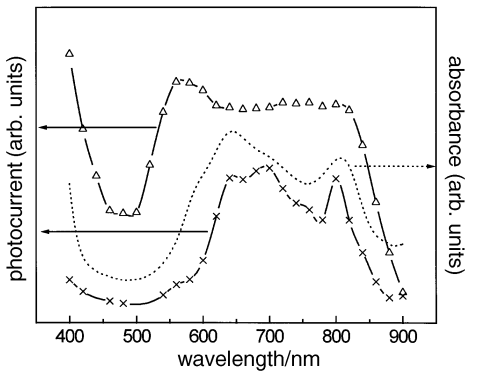

Fig. 4 Short-circuit photocurrent action spectra illuminated through ITO (△) and gold contact (×) of a ITO|F_{16}PcZn[240 nm]|air|Au device stored under air for 48 hours. The sample was illuminated either with 10^{15} photons s^{-1} cm^{-2} (ITO) or with 10^{14} photons s^{-1} cm^{-2} (gold) incident on the organic layer. The dotted line corresponds to the solid state absorption spectrum.

identical as possible six ITO|F_{16}PcZn devices were prepared in the same deposition step to ensure the same vacuum conditions and layer properties which were then stored under air before Au deposition (ITO|F_{16}PcZn[240 nm],air|Au). After two days storage the photovoltage had already reached a maximum value of −500 mV. From then on a continuous decrease in photovoltage was observed. Without the metal film hindering the uptake of O_2 in this geometry it took only three weeks until the photovoltage decreased to −80 mV again. Basically the same change was observed as in Fig. 3(a) but occurring considerably faster.

The spectral distributions of photocurrent action under polarization and short circuit condition (I_{SC}) at an ITO|F_{16}PcZn[240 nm],air|Au device exposed to air for 2 days (48 h) are shown in Fig. 4. Illumination through the Au electrode led to short circuit action spectra similar in shape to the F_{16}PcZn solid state absorption spectrum. Light which is strongly absorbed near the Au contact contributed most efficiently to the photocurrent. On the other hand, the photocurrent under illumination through ITO showed maxima at wavelengths of intermediate absorption by F_{16}PcZn. This is known as the optical filter effect, typically found in materials with high absorption coefficients if only light of medium and weak absorption is able to penetrate deep into the bulk causing photocurrent peaks at the slope of the absorption spectrum.[27] Both spectra therefore reveal that the photoactive area is located on the Au side rather than at the ITO side of the sample.

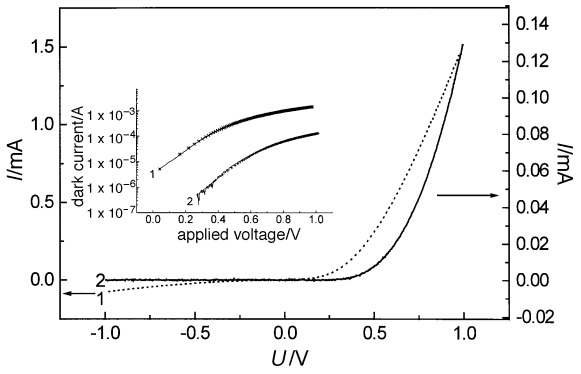

Fig. 5 Current–voltage characteristics of ITO|F_{16}PcZn[150 nm]|In as prepared (1) and stored under air for 2 h (2) devices. The inset shows a plot of ln *I versus V* for forward bias (—) and a fit (×) based on parameters obtained from a modified Schottky equation for the conditions (1,2) as seen in the main diagram.

(d) ITO|F_{16}PcZn|In devices

This device clearly exhibits rectifying characteristics at the contact with In under all conditions of our experiments. From a value of 17 in vacuum (Fig. 5, plot 1) the rectification ratio $r_{rf,\pm 1V}$ corresponding to ± 67 kV cm^{-1} increases to 640 (Fig. 5, plot 2) during exposure to air. More detailed analysis of $I(U)$ plots allows a short discussion of the mechanism of charge transport over the barrier. If the classical Schottky equation is modified by introducing a series resistance[28]

$$I_{\text{forward}} = I_0 \exp \frac{[e(V-IR)]}{nkT} \quad (2)$$

is obtained where I_{forward} is the current of the forward biased device, I_0 the saturation current, e the charge of an electron, n a dimensionless ideality factor, k Boltzmann's constant, V the applied potential, R the series resistance and T the absolute temperature. A good fit was obtained over the investigated range up to +1 V for devices as prepared in HV with fitting parameters $n=3.4$, $I_0=3.2\times10^{-6}$ A, $R_s=303$ Ω (Fig. 5 inset, plot 1), as well as for devices stored in air for 2 h with $n=3.1$, $I_0=4.8\times10^{-8}$ A and $R_s=2204$ Ω (Fig. 5 inset, plot 2). This example clearly underlines the rather high series resistance that has to be taken into account in F_{16}PcZn layers to characterize the diode behavior in the forward direction. The corresponding barrier height[28] ϕ_b was calculated to be 0.6 V for devices as prepared and as 0.7 V for devices exposed to air for 2 h. If the values of R_s are used to calculate the corresponding specific conductivities of the sample, values of $\sigma_{301K,\ \text{as prepared}}=4.1\times10^{-7}$ S cm^{-1} and $\sigma_{301K,\ \text{air}}=5.6\times10^{-8}$ S cm^{-1} are obtained. These values are higher than those determined in contact with Au and ITO (previous section) by three to four orders of magnitude. Such an increase can only be explained by the creation of additional charge carriers in F_{16}PcZn by interaction with In.

(e) ITO|F_{16}PcZn|PcZn|Au devices

For ITO|F_{16}PcZn|PcZn|Au we measured a value of $U_{OC}\approx+70$ mV [Fig. 3(c)] and a corresponding short circuit current of $I_{SC}=-0.4$ μA when measured in vacuum as prepared and illuminated with white light through ITO. Photocurrent action spectroscopy was again used to determine the site of charge carrier generation. The shape of the photocurrent action spectrum as measured in vacuum was directly correlated with the thickness of the first organic layer that the light had to pass. Fig. 6 (solid symbols) is a depiction of spectra (negative photocurrents) obtained through ITO at ITO|F_{16}PcZn|PcZn|Au cells with different thicknesses of the F_{16}PcZn layer. Devices with a rather thin layer of F_{16}PcZn

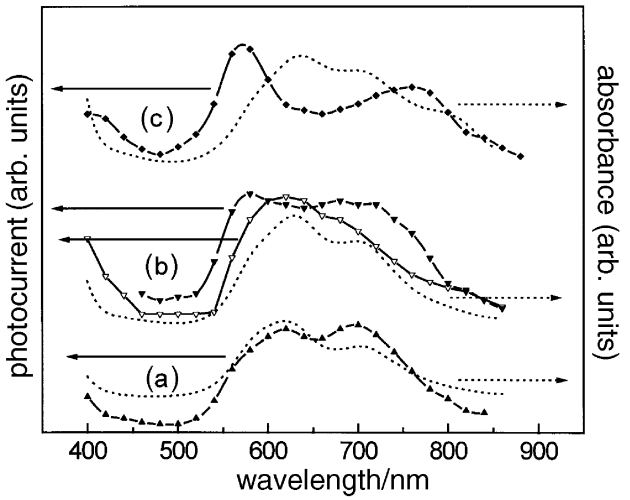

Fig. 6 Short-circuit photocurrent spectra of devices as prepared in vacuum: ITO|F_{16}PcZn[30 nm]|PcZn[160 nm]|Au (a,▲), ITO|F_{16}PcZn[90 nm]|PcZn[90 nm]|Au (b,▼) and ITO|F_{16}PcZn[250 nm]|PcZn[90 nm]|Au (c,◆). All devices were illuminated through the ITO side with a constant 10^{15} photons s^{-1} cm^{-2}, a NEGATIVE current is plotted upwards. The dotted line corresponds to the solid state absorption spectrum of each device. In part b (▽) the photocurrent of ITO|F_{16}PcZn[90 nm]|PcZn[90 nm]|Au is included after 48 h of exposure to air, POSITIVE currents plotted upwards.

(30 nm) showed peaks in the same position as the solid state VIS spectrum of the device [Fig. 6(a), ▲]. Light strongly absorbed in both layers contributed significantly. Devices with a 90 nm F_{16}PcZn layer [Fig. 6(b), ▼] resulted in action spectra with photocurrent maxima shifted toward the slopes of the solid state VIS spectrum. This effect was increased by the choice of an even thicker F_{16}PcZn layer [250 nm, Fig. 6(c), ◆] where the maximum contribution was found for light where the film absorbance reached 50% of the maximum value as typical for perfect optical filters. This light offered the optimum compromise of deep penetration and still considerable absorbance. Consistently a photocurrent minimum was observed for the wavelength of maximum absorbance. The observed behavior points towards F_{16}PcZn|PcZn as the active junction with two non-active contacts ITO|F_{16}PcZn and PcZn|Au as expected, since both ITO|F_{16}PcZn and PcZn|Au had been shown to be ohmic, as described above.

Both the open circuit voltage and the sign of the photocurrent changed after exposure to air [Fig. 3(c)]. After exposure to air (positive photocurrents) the photocurrent action spectrum measured under illumination through ITO|F_{16}PcZn closely resembles that of film absorbance [Fig. 6(b), ▽]. This is not the case when illuminated through the gold back electrode for Au|PcZn. From the observed directions of optical filtering it is evident that the active area is shifted into the F_{16}PcZn layer. Under white light [Fig. 3(c)] a negative photovoltage of about −320 mV was reached after a period of 1700 h (2 months). Samples stored for 4000 h (5.5 months) in air showed a decreased photovoltage of about −180 mV. Interestingly after one year in air the photovoltage again (compare ITO|F_{16}PcZn|Au) approached a value comparable in sign and magnitude to freshly prepared devices in vacuum. After this period no difference in shape was found in the photocurrent action spectra when compared to spectra initially obtained in vacuum. After such extended exposure the photoactive area had swept back to the F_{16}PcZn|PcZn interface.

(f) Ultraviolet photoelectron spectroscopy (UPS)

After the HOMO–LUMO gaps had been estimated from optical absorption spectra [Fig. 1(b)] UPS was performed to determine the absolute positions of the frontier orbitals. During deposition of the metal complexes spectra shifted in energy due to a change in work function from the bare Au surface to surfaces with varying proportions of Au and organic material to reach a constant position when a surface of the pure organic was reached at a thickness of 5–20 nm. The HOMO was then found to be positioned at −6.9 eV *vs.* vacuum for F_{16}PcZn [Fig. 7(a)] and at −5.3 eV *vs.* vacuum for PcZn [Fig. 7(d)]. The position of the HOMO in Scheme 1 is based on these results.

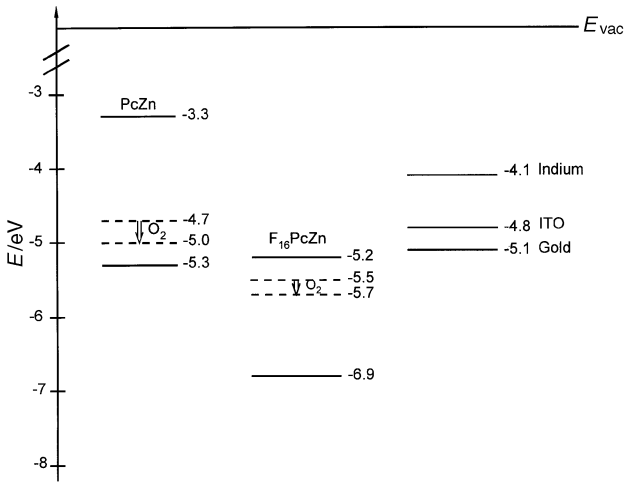

Scheme 1 Energy diagram of F_{16}PcZn and PcZn as determined in this work compared to values of ITO, gold and indium from the literature[42,43]

To analyse the alignment of energy levels during junction formation, spectra were also obtained during growth of PcZn on top of a film of pure F_{16}PcZn. Fig. 7(a)–(c) show a sequence of spectra typical of heterojunction formation of the two materials. The escape depth of electrons travelling with a kinetic energy of about 10 eV will also be rather small in organic materials and can be estimated as about 1 nm.[29,30] Therefore during deposition of PcZn, emission from the HOMO of F_{16}PcZn is still collected but attenuated considerably by inelastic scattering of photoelectrons (contributing to the large secondary electron emission signal) and some absorption of HeI photons in the top layer. This is seen in Fig. 7(b) and (c), accompanied by a signal of the PcZn HOMO growing in.

None of the bands in the heterojunction is found at an energy typical of the corresponding material in a single layer.

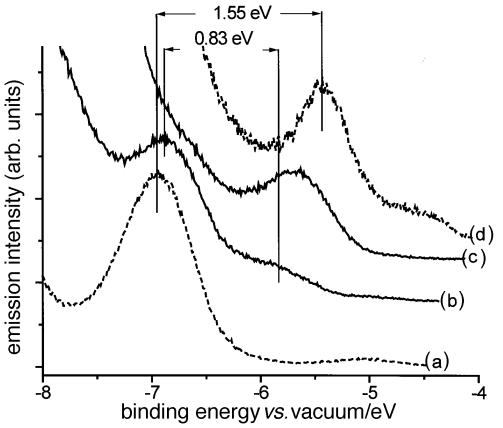

Fig. 7 HeI UPS spectra in vacuum of pure films (– – –) on Au (a) 20.1 nm F_{16}PcZn and (d) 6.8 nm PcZn as well as of the organic heterojunction (—) after deposition of 0.4 nm PcZn (b) and 0.7 nm PcZn (c) on top of 20.1 nm of F_{16}PcZn

These shifts are caused by the fact that the apparent work function is averaged according to the materials present at the surface, as expected for rather thin films (islands) of PcZn leading to an apparent shift to smaller binding energy for the HOMO of F_{16}PcZn and to larger binding energy for the HOMO of PcZn. This shift is clearly seen in Fig. 8 in which the orbital positions for the highest (HOMO) and second-highest (SOMO) occupied orbitals are depicted as obtained from a full series of experiments on PcZn deposited on top of F_{16}PcZn. Within the margin of error, which is caused by the problems of finding a good Gaussian fit to small shoulders in the emission signal, a parallel shift is found for all four orbitals under investigation. This is expected from the postulated shift in work function of the overall sample.

Discussion

The solid state spectrum of PcZn corresponds to the α structure [Fig. 1(b)]. It is characterized by the Davydov splitting of 86 nm between the two branches of the exciton manifold which is in agreement with results taken from the literature.[31] This would correspond to a splitting energy of 0.07 eV for each branch. The spectrum obtained for the film of F_{16}PcZn in the solid state is significantly broader which points towards the presence of a mixture of different modifications.[32] This hypothesis is supported by experiments at varying substrate temperatures during deposition. At higher temperatures the intensity of the band at 814 nm clearly increases at the cost of those at smaller wavelengths.[33] The observation that there is no corresponding band that far on the blue side of the solution band indicates that the transition dipoles of the molecules leading to the transition at 814 nm are oriented head to tail.[23] The splitting energy of this band therefore has to be determined from the difference to the band in solution which yields 0.29 eV, considerably larger than the value of PcZn. Following the model of Kasha the rather large splitting energy points towards a quite strong interaction between two F_{16}PcZn molecules in the unit cell.[22,23] Interactions in organic crystals are known to be of the van der Waals type.[32] Obviously the high electronegativity of the 16 fluorine atoms leads to the preferred head to tail arrangement at a higher interaction energy for F_{16}PcZn when compared to PcZn.

To explain the presented results of organic|metal and organic|organic devices based on energetic considerations it is firstly necessary to summarize the relevant positions of the Fermi level and frontier orbitals of thin films as prepared in vacuum (Scheme 1). In a subsequent step, changes in the observed device parameters caused by exposure to air will be discussed.

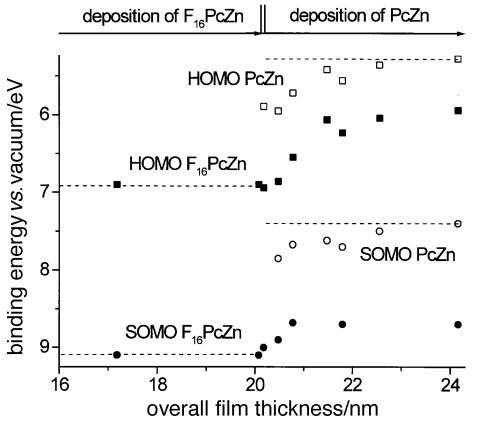

Fig. 8 Orbital positions of the highest occupied molecular orbital (HOMO, squares) and the second highest occupied molecular orbital (SOMO, circles) of F_{16}PcZn (solid symbols) and of PcZn (open symbols) as determined from He_I UPS of the materials in a junction of PcZn deposited on top of 20.1 nm of F_{16}PcZn. Bulk binding energies are included as dashed lines.

The HOMO positions are obtained from the UPS experiments (−6.9 eV for F_{16}PcZn, −5.3 eV for PcZn), the LUMO positions are estimated by adding the energy corresponding to the optical transition of lowest energy (1.5 eV for F_{16}PcZn, 1.8 eV for PcZn) and a molecular exciton dissociation energy of 0.2 eV each. Recently it was shown that the Kelvin probe method (KPM) is well suited for the determination of Fermi level positions in vapor deposited organic thin films and $E_F = -4.7$ eV was determined for PcZn and $E_F = -5.5$ eV for F_{16}PcZn in vacuum.[34] It follows from the given data that PcZn as prepared in vacuum should show weak p-type conductivity correlated with a Fermi level position of about 0.4 eV below the middle of the band gap, 0.6 eV above the HOMO. These results are in good agreement with the thermal activation energy for electrical conduction of 0.55 eV as we reported earlier for a film on a microelectrode array,[11] and the value of 0.7 eV as found in this study for Au|PcZn|Au sandwich devices as prepared in vacuum. The Fermi level of F_{16}PcZn is located 0.55 eV above the middle of the band gap, about 0.3 eV below the LUMO. A thermal activation energy of 0.2 eV measured for ITO,Au|F_{16}PcZn|Au devices in vacuum underlines this result. Excess electrons in unoccupied orbitals should therefore determine the electrical properties of F_{16}PcZn films (n-type conductivity), which is confirmed by independent experiments.[13] We generally see such an influence of electronegative substituents on the observed conduction type.[2,10–14] The molecules are less easily oxidized but more easily reduced when compared to Pc and therefore it is reasonable that PcZn is interacting with residual acceptor molecules like O_2, and F_{16}PcZn with residual donor molecules even of very low concentration. Such impurities are present during vapor deposition of phthalocyanines, even after purification by zone sublimation.

In order to reach thermodynamic equilibrium (constant electrochemical potential and hence E_F) in a junction of different materials an original difference in E_F has to be balanced by electron transfer from the phase of higher position to the phase of lower position or by hole transfer in the opposite direction. Therefore, owing to the simple model of different work functions, n-type conductors should exhibit ohmic contacts to metals with lower and rectifying contacts to metals with higher work functions (electron accumulation in the first, electron depletion in the second case). For a p-type material the opposite is expected (hole depletion, hole accumulation). In this approach surface states and traps in the bulk material, however, were not taken into account. Using these simple rules ohmic behavior can be predicted for ITO|F_{16}PcZn|Au devices (Scheme 1). This is in good agreement with the experimental results for devices as prepared in vacuum (Fig. 2 inset). To reach equilibrium electrons have to flow from gold and ITO into F_{16}PcZn. This process leads to a surface electron accumulation layer of non-localized charge carriers which contributes to an unhindered charge transfer through the interface. Only a small number of imperfections, probably due to localized states, are detected by the comparably small photovoltage in vacuum [Fig. 3(a)]. As a result the proposed simple work function model makes it possible to explain the observed dark electrical properties of F_{16}PcZn in contact with Au and ITO. As expected from the work functions, PcZn|Au as well as PcZn|ITO contacts also exhibit ohmic behavior in vacuum and under air.

After exposure to air the electrical conductivity in PcZn layers increased while that in F_{16}PcZn films decreased. Oxygen acts, as expected, like a strong electron acceptor leading to a partial oxidation of PcZn. This leads to an increase of charge concentration in PcZn (p-type). On the other hand, oxygen decreases the number of free charge carriers in F_{16}PcZn (n-type) by compensation of donor levels. If the Boltzmann

approximation is used for the distribution of occupied states in the materials and if changes in σ are assumed to be directly correlated to changes in the concentration of charge carriers (neglecting any influence on trap levels) the values of σ as stated above can be used to estimate changes in E_F. Following this simplifying approach, E_F in the organic materials was shifted by about 0.3 eV towards lower energies to -5.0 eV for PcZn and by about 0.2 eV to -5.7 eV for F_{16}PcZn after several months of exposure to air (arrows in Scheme 1). This result is in good agreement with the observed $E_A = 0.3$ eV and 0.4 eV of σ obtained at films of PcZn[2] and F_{16}PcZn as reported above which had been exposed to O_2 prior to characterization in vacuum.

Not only changes in the dark conductivity, but also changes in U_{OC} after different exposure to air, were observed for ITO|F_{16}PcZn|Au devices [Fig. 3(a)]. In addition, it is of crucial importance whether the top gold electrode is deposited under HV in one step without breaking the vacuum, or after air exposure of the organic film. Qualitatively we observed the same behavior for each case, but the timescale of changes is strongly affected. In both cases the photovoltage is directly correlated to the exposure to oxygen. The results as presented in Fig. 3(a) and (b) show that the diffusion of oxygen into the film is responsible for the observed changes. For devices exposed to air for intermediate periods of time without prior deposition of the gold top electrode the diffusion is facilitated and consequently it took only 48 h to reach the maximum photovoltage. For devices entirely produced in vacuum a 35-fold longer storage time is required to reach a photovoltage of similar size. After this maximum was reached the photovoltage decreased to the original value found at the beginning, before exposure to air.

A parallel change in time was observed in the dark current–voltage plots. Starting from a symmetrical curve (plot 1 in Fig. 2) before exposure, a current was measured for devices exposed to air for 880 h (plot 2 in Fig. 2) which was about 20 times higher in the forward direction (ITO polarized negatively) than that in the reverse direction. After a storage period of 4500 h in air this rectification ratio $r_{rf\pm1V}$ decreased to 3 (plot 3 in Fig. 2). These changes can no longer be explained by the model of different work functions. Instead rather localized chemical reactions have to be assumed to discuss the results. Due to the adsorption of electron accepting oxygen, negatively charged surface states of reduced oxygen at the Au|F_{16}PcZn interface and positively ionized localized donor levels in the bulk of F_{16}PcZn are formed [Scheme 2(a)]. These establish an electrical field directed from the positive to the negative ionized levels. This field explains the unsymmetrical current–voltage plots as well as the direction of exciton dissociation leading to the photovoltage as observed under illumination. Recently a similar influence of oxygen on the rectification ratio of PbPc sandwiched between two gold electrodes was reported.[35,36] After the surface reaction is complete O_2 diffuses and reacts with the bulk F_{16}PcZn as σ decreases continuously [Fig. 2, Scheme 2(b)] while the photovoltage [Fig. 3(a) and (b)] as well as r_{rf} at first increase when the field extends further into the film of F_{16}PcZn and then decrease when the gradient levels off as soon as the whole film reacts. At that time a symmetrical situation is established, again characterized by a symmetrical current–voltage curve and a negligible photovoltage [Scheme 2(c)]. In contrast to p-type PbPc, oxygen does not oxidize F_{16}PcZn because of the strong frontier orbital lowering. It instead leads to an electron concentration gradient due to majority charge carrier trapping and compensated ionized donor sites. Photoconductivity transient studies on F_{16}PcZn thin films underline the existence of such deep oxygen traps.[13] Spoken in terms of energy levels this proposed mechanism leads to a Fermi level position in the bulk and near the bottom electrode which remains nearly unchanged after short air contamination periods while its position is already shifted

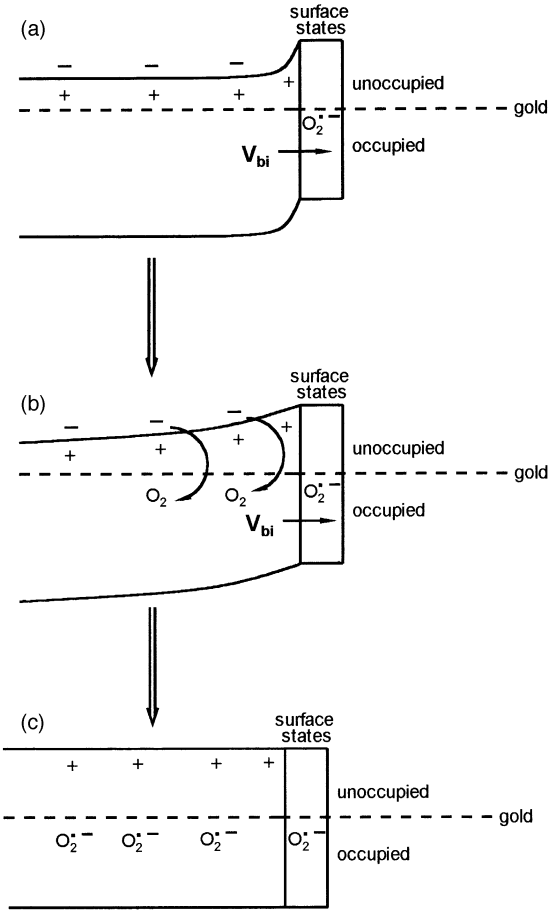

Scheme 2 Proposed model of surface states and oxygen concentration gradient in F_{16}PcZn layers in contact with gold during increasing (a,b,c) exposure to air

toward the middle of the band gap in the near surface region. We think this is the reason for the observed changes in the open circuit voltage and r_{rf}. After sufficiently long storage periods in air [Fig. 3(a) and (b)] both open circuit voltage and charge carrier concentration gradients disappear which goes along with a symmetrical oxygen distribution across the F_{16}PcZn layer [Scheme 2(c)]. In summary, one can say that the rectification ratio and open circuit voltage are exclusively determined by oxygen diffusion into the film independent of the work functions of the electrode materials but reacting with the dopant molecules.

A similar series of reactions has to be assumed when discussing the properties of F_{16}PcZn|indium. In this case a quite complex situation is caused by reactions of the metal itself. Examination of the energy levels in Scheme 1 reveals an expectation of ohmic behavior of the contact as electrons should be injected from In into F_{16}PcZn. But unsymmetrical current–voltage characteristics of devices as prepared (Fig. 5) already differ from this assumption by showing blocking behavior. Nevertheless thermal equilibrium requires electron transfer from In to F_{16}PcZn. These charges, however, obviously are not mobile and are located at the F_{16}PcZn|In interface. In has high reducing power while F_{16}PcZn is a strong oxidizer. This combination seems to lead to direct electron transfer by chemical interaction of the two reactants which can generally be simplified as:

$$3[F_{16}PcZn]|\text{indium} \rightarrow 3[F_{16}PcZn]^{\cdot -}|\text{indium}^{3+}$$

Transferred electrons would therefore be located in deep electron traps. Chemical interaction of In and Al with organic molecules has been detected by synchrotron radiation photo-

emission spectroscopy for electron accepting 3,4,9,10-perylenetetracarboxylic dianhydride (PTCDA)[37] as well as for TCNQ[38,39] and a strong influence on the electrical properties was found. Direct chemical interaction of In and F_{16}PcZn is further supported by a number of fluorine complexes for In^{3+} and In^{5+}.[40] These reactions lead to an electrical field with a negative charge in F_{16}PcZn and the positive charge for In which explains the present results in ITO|F_{16}PcZn|In. A positive potential at ITO leads to a compensation of the built-in electrical field and therefore the current flows in the forward direction. At negative polarization of ITO the internal field is enhanced and the current is blocked. Due to the strongly different redox properties of F_{16}PcZn towards In when compared to O_2, the direction of this built-in electrical field is in the opposite direction when compared to the field in F_{16}PcZn|Au devices under the influence of O_2. Although the nature of barrier formation is quite different from classical ideal devices, the current–voltage characteristics in the forward direction of F_{16}PcZn|In are rather well described by a modified Schottky equation (Fig. 5). From that analysis we further have to conclude that this reaction with In also extends into the bulk of F_{16}PcZn as σ calculated for the film by far exceeds the value as observed in ohmic contacts with Au. Different from the surface interaction where localized charges dominate the reaction in the bulk of F_{16}PcZn, the reaction with In obviously leads to an additional concentration of mobile charge carriers which contribute to σ.

After exposure to air the rectification ratio increased with decreasing conductivity and current in the forward direction (Fig. 5, case 2). The increase in r_{rf} points towards an additional surface charge caused by electron transfer from indium to oxygen which increases the strength of the built-in electrical field. The presence of O_2 seems to be of general importance to obtain high rectification ratios in organic contacts to In or Al, as this was also observed for PcZn|Al devices stored under air compared with those measured as prepared in vacuum.[41] The detailed analysis of the current–voltage characteristics (Fig. 5) confirms the improved diode behavior but also reveals the increased resistance in series with the diode. This could either be caused by an oxide-like surface species or by a decreased σ in the bulk of the F_{16}PcZn phase. From the experiments at F_{16}PcZn|Au under exposure to air we know that O_2 penetrated deeply into F_{16}PcZn and compensated donor levels. Therefore the same reaction has to be taken into account in F_{16}PcZn|In. Indium, as a strong reducing agent, would be the predominant donor to be compensated. By this reaction σ decreases significantly as most of the charge carriers generated in the bulk interaction with In are no longer present. In spite of the high interaction potential for O_2 with In this reaction was found to take a considerable time. Even after 2 h in air σ is still about two magnitudes of order higher than the conductivity of F_{16}PcZn in interaction with donor molecules from the deposition as measured in the contact with Au prior to air exposure. This further underlines the bulk character of the reactions of F_{16}PcZn films both with O_2 and In and thereby indicates an interesting potential for doping organic acceptors with In, but also shows the need to efficiently exclude air in order to avoid compensation.

The third example to be considered for direct chemical interaction of two materials as well as bulk interaction with mobile species is found in the results at PcZn|F_{16}PcZn. ITO top and gold bottom electrodes were chosen for PcZn|F_{16}PcZn devices to make sure that the opto-electrical properties are exclusively determined by the organic junction properties as ohmic behavior was shown for ITO|F_{16}PcZn and PcZn|Au devices as prepared in vacuum. Electron transfer from the material with the smaller work function (PcZn) to the material with the larger work function (F_{16}PcZn) has to occur to reach thermal equilibrium in the contact (Scheme 1). An internal electrical field arises from localized states of the character $PcZn^+$ and $F_{16}PcZn^-$. Scheme 3 depicts the general situation at the PcZn|F_{16}PcZn junction in thermal equilibrium without claiming detailed characterization. The built-in field is shown by the arrow V_{bi} directed from positive localized ionized states in PcZn to negative charged states in F_{16}PcZn. Positive potential applied at the ITO (F_{16}PcZn) electrode corresponds to compensation of the built-in internal electrical field and thereby unhindered current as seen in the experiment. Under illumination excitons are formed and dissociate at the PcZn|F_{16}PcZn interface in the V_{bi} region to yield additional electrons in PcZn and holes in F_{16}PcZn, as also indicated in Scheme 3. This process leads to the observed U_{OC} in vacuum which is positive at F_{16}PcZn (ITO) and negative at PcZn (Au). The dependence of the open circuit voltage on the light intensity indicates that U_{OC} can not be altered above +70 mV with increasing light intensity. This value is considerably smaller than the maximum possible value of +700 mV as can be expected from the difference in Fermi energies of 0.7 eV (Scheme 1). The separated photo-generated charge carriers are not able to establish an electrical field strong enough to balance V_{bi}. Electrons are accumulated at the surface of F_{16}PcZn due to the downbending of the LUMO levels (arrow 1 in Scheme 3). Holes are accumulated at the surface of PcZn due to the upward bending of the HOMO levels (arrow 2 in Scheme 3). Holes in F_{16}PcZn and electrons in PcZn diffuse into the bulk materials. The accumulation processes are responsible for a high probability for radiationless charge carrier recombination (arrows 3 in Scheme 3). As a consequence only an insufficiently small concentration of free holes (F_{16}PcZn) or electrons (PcZn) is generated.

If F_{16}PcZn|PcZn devices are exposed to air the polarity of U_{OC} changes in sign [Fig. 3(c)]. This is again explained by subsequent reaction of the films with O_2. PcZn will be the first layer to be reacted by lowering E_F beginning from the surface towards the interface with F_{16}PcZn leading to a decrease in the potential drop across the whole structure and hence in U_{OC}. As soon as F_{16}PcZn starts to react the unsymmetrical doping profile, as already discussed for F_{16}PcZn|Au, has to be expected and it leads to a further decrease in U_{OC}. As the time dependence and the size of U_{OC} both resemble those found for F_{16}PcZn|Au it can even be assumed that the influence of O_2 on PcZn can be neglected and that U_{OC} is determined solely by the subsequent reaction of O_2 with F_{16}PcZn. As discussed before (Scheme 1) the Fermi level positions of both materials are lowered by approximately the same amount due to the influence of O_2 after equilibrium is reached with O_2 after sufficient storage periods of several months. If the interaction of F_{16}PcZn and PcZn at their interface remains mainly

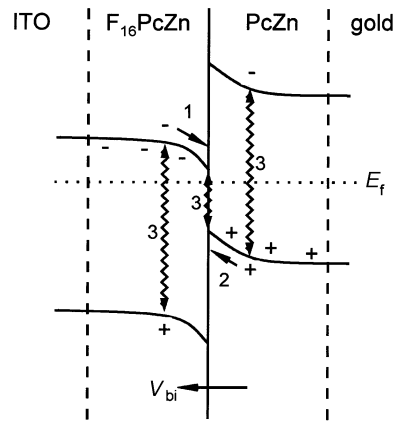

Scheme 3 Proposed energy diagram for the contact F_{16}PcZn|PcZn after interfacial charge transfer in vacuum. The preferred direction for minorities following exciton dissociation are shown for electrons (1) and holes (2) as well as recombination pathways (3).

unaffected by O_2, no change in polarity would be expected for that case as confirmed by our experiment [Fig. 3(c)]. As our model qualitatively explains the behavior of the device under the different conditions we can state that the negative photovoltage is not determined by the F_{16}PcZn|PcZn interface but by the unsymmetrical doping/compensation profile in F_{16}PcZn as also found in F_{16}PcZn|Au (Scheme 2) and F_{16}PcZn|In.

The *in situ* UPS analysis of the heterojunction allows us to discuss the surface interaction of PcZn and F_{16}PcZn in more detail. If a typical space-charge layer would have been formed, a difference in orbital energies of the two materials would be evident, which changes with the thickness of the deposited material. This was not the case in the present study, as seen in Fig. 8, as the bulk value of PcZn is already reached at an average thickness of 4 nm. When a thin film of PcZn was deposited on top of F_{16}PcZn to detect emission from both materials interfacing each other, a shift was observed in the positions of all bands which was caused by a drift in work function of the overall sample, but the relative positions of the orbitals remained constant, *i.e.* there is no significant change of the position of $HOMO_{PcZn}$ or $SOMO_{PcZn}$ with respect to the $HOMO_{F_{16}PcZn}$ or $SOMO_{F_{16}PcZn}$. No macroscopic space-charge layer is formed because no relative shift of the two sets of orbitals with film thickness of PcZn as a result of charge transfer could be measured.

Nevertheless, the establishment of equilibrium between the two samples is clearly observed as can be seen from the observation that the difference of HOMO energies in the heterojunction was considerably smaller [0.83 eV, Fig. 7(b)] than the difference as determined from single films [1.55 eV, Fig. 7(a), (d)]. The same statement holds for the SOMO as well as for even deeper-lying orbitals. This finding points towards establishment of thermodynamic equilibrium at the interface as parallel emission from independent species of PcZn and F_{16}PcZn would lead to the difference of 1.55 eV [Fig. 7(a), (d)]. If the Fermi energies of the materials as measured *in situ* by KSM[34] are aligned in the junction of the materials (Scheme 1), a HOMO separation in the bulk films of $(E_{F,F_{16}PcZn}-E_{HOMO,F_{16}PcZn})-(E_{F,PcZn}-E_{HOMO,PcZn})=$ 1.4 eV − 0.6 eV = 0.8 eV is calculated which is in perfect agreement with the experimental value of 0.83 eV. This establishment of equilibrium of F_{16}PcZn and PcZn during deposition of PcZn on top of F_{16}PcZn clearly demands an interfacial charge transfer due to the initial difference in energy levels as a fundamental prerequisite. On the other hand, no formation of a macroscopic space-charge layer was observed (Fig. 8). From these findings it becomes clear that the orbital positions were determined in the volume of each material which did not participate in the charge transfer reaction and that the signals originating from the molecules chemically interacting in the charge transfer at the interface obviously were too weak and inhomogenous to be detected.

Conclusions

n-Type conductivity has been confirmed for F_{16}PcZn. When discussing the rectification found in the dark and the photovoltage observed under illumination in a series of junctions involving F_{16}PcZn the importance of direct chemical interaction with a different kind of molecular semiconductor (PcZn) or with a reactive metal electrode (In) is evident. UPS provided us with a detailed analysis of the junction of PcZn for which the establishment of thermodynamic equilibrium in the interface could be proven. Interaction of F_{16}PcZn with In leads to a larger increase in the concentration of free charges. These as well as those originating from reaction with donor molecules during film growth are compensated by O_2 when films are exposed to air. The slow diffusion and reaction of In or O_2 with F_{16}PcZn establishes a largely unsymmetrical situation with respect to dopant profile and hence Fermi energy as a result of this non-equilibrium, leading to the observed electrical properties in the dark and under illumination.

The authors are grateful to N. I. Jaeger (University of Bremen, Germany) for stimulating discussions and valuable advice and to K. W. Nebesny, P. Lee and M. Anderson (University of Arizona, Tucson, AZ) for support in the UPS experiments as well as the Center of Advanced Multifunctional Polymers and Molecules (CAMP, ONR/DOD), the Deutsche Forschungsgemeinschaft (DFG Schl 340/3-1,2) and the Bremen Government (55 2/11) for financial support.

References

1 J. Simon and J.-J. Andre, in *Molecular Semiconductors*, Springer Verlag, Berlin, 1986.
2 J.-P. Meyer, D. Schlettwein, D. Wöhrle and N. I. Jaeger, *Thin Solid Films*, 1995, **258**, 317.
3 D. Wöhrle and D. Meissner, *Adv. Mater.*, 1991, **3**, 129.
4 D. Wöhrle, L. Kreienhoop, G. Schnurpfeil, J. Elbe, B. Tennigkeit, S. Hiller and D. Schlettwein, *J. Mater. Chem.*, 1995, **5**, 1819.
5 D. Wöhrle, L. Kreienhoop and D. Schlettwein, in *Phthalocyanines*, ed. C. C. Leznov and A. P. B. Lever, VCH Publications, 1995, vol. 4.
6 W. J. Pietro, *Adv. Mater.*, 1994, **6**, 239.
7 A. Wilson and J. D. Wright, *Mol. Cryst. Liq. Cryst.*, 1992, **211**, 321.
8 K. Y. Law, *Chem. Rev.*, 1993, **93**, 449.
9 R. Signerski, J. Kalinowski, I. Davoli and S. Stizza, *Phys. Status Solidi A*, 1991, **125**, 597.
10 D. Schlettwein and N. R. Armstrong, *J. Phys. Chem.*, 1994, **98**, 11771.
11 D. Schlettwein, N. R. Armstrong, P. A. Lee and K. W. Nebesny, *Mol. Cryst. Liq. Cryst.*, 1994, **253**, 161.
12 D. Schlettwein, D. Wöhrle, E. Karmann and U. Melville, *Chem. Mater.*, 1994, **6**, 3.
13 E. Karmann, J.-P. Meyer, D. Schlettwein, N. I. Jaeger, M. Anderson, A. Schmidt and N. R. Armstrong, *Mol. Cryst. Liq. Cryst.*, 1996, **283**, 283.
14 J.-P. Meyer and D. Schlettwein, *Adv. Mater. Opt. Electron.*, 1996, **6**, 239.
15 A. Schmidt, M. L. Anderson, P. A. Lee, N. R. Armstrong, G. Schnurpfeil, S. Hiller, D. Schlettwein and D. Wöhrle, *J. Phys. Chem.*, submitted.
16 T. L. Anderson, G. C. Komplin and W. J. Pietro, *J. Phys. Chem.*, 1993, **97**, 6577.
17 E. Allemann, N. Brasseur, O. Benrezzak, J. Rousseau, S. V. Kudrevich, R. W. Boyle, J.-C. Leroux, R. Gurny and J. E. van Lier, *J. Pharm. Pharmacol.*, 1995, **47**, 382.
18 J. Ouyang, K. Shigehara, A. Yamada and F. C. Anson, *J. Electroanal. Chem.*, 1991, **297**, 484.
19 D. Schlettwein, K. Hesse and N. I. Jaeger, manuscript in preparation.
20 J. M. Birchall, R. N. Haszeldine and J. O. Morley, *J. Chem. Soc. C*, 1970, 2667.
21 E. D. Olsen, in *Modern Optical Methods of Analysis*, McGraw-Hill, New York, 1975.
22 L.-K. Chau, C. D. England, S. Chen and N. R. Armstrong, *J. Phys. Chem.*, 1993, **97**, 2699.
23 R. M. Hochstrasser and M. Kasha, *Photochem. Photobiol.*, 1964, **3**, 317.
24 A. S. Davidov, in *Theory of Molecular Excitons*, McGraw Hill, New York, 1962.
25 J. J. Andre, J. Simon, R. Even, B. Boudjema, G. Guillaud and M. Maitrot, *Synth. Met.*, 1987, **18**, 683.
26 N. El-Khatib, B. Boudjema, G. Guillaud, M. Maitrot and H. Chermette, *J. Less-Common Met.*, 1988, **143**, 101.
27 S. Günster, S. Siebentritt, J. Elbe, L. Kreienhoop, B. Tennigkeit, D. Wöhrle, R. Memming and D. Meissner, *Mol. Cryst. Liq. Cryst.*, 1992, **218**, 117.
28 S. M. Sze, in *Physics of Semiconductor Devices*, Wiley, New York, 1981.
29 D. Briggs, in *Practical Surface Analysis*, Wiley, Chichester, 1990.
30 J. B. Hudson, in *Surface Science—An Introduction*, Butterworth/Heinemann, Stoneham, 1992.
31 E. A. Lucia and F. D. Verderame, *J. Chem. Phys.*, 1968, **48**, 2674.
32 A. Schmidt, L. K. Chau, A. Back and N. R. Armstrong, in *Phthalocyanines*, ed. C. C. Leznoff and A. P. B. Lever, VCH Publications, 1995, vol. 4.

33 D. Schlettwein, H. Graaf and D. Wöhrle, manuscript in preparation.
34 M. Pfeiffer, K. Leo and N. Karl, *J. Appl. Phys.*, 1996, **80**, 6880.
35 J. Kaspar, I. Emmer and R. A. Collins, *Int. J. Electron.*, 1994, **76**, 793.
36 R. A. Collins, A. K. Abass and M. Pfeiffer, *Int. J. Electron.*, 1994, **76**, 787.
37 Y. Hirose, A. Kahn, V. Aristov, P. Soukiassian, V. Bulovic and S. R. Forrest, *Phys. Rev. B*, 1996, **54**, 13748.
38 M. Maitrot, G. Guillaud, B. Boudjema, J. J. Andre and S. Simon, *J. Appl. Phys.*, 1986, **60**, 2396.
39 T. Patterson, J. Pankow and N. R. Armstrong, *Langmuir*, 1991, **7**, 3160.
40 J. W. Mellor, in *Comprehensive Practice on Inorganic and Theoretical Chemistry*, Longmans, London, 1961, vol. 5.
41 M. Martin, J.-J. Andre and J. Simon, *Appl. Phys.*, 1983, **54**, 2792.
42 N. Balasubramaniam and A. J. Subrahmanyam, *Electrochem. Soc.*, 1991, **138**, 322.
43 *CRC Handbook of Physics and Chemistry*, ed. D. R. Lide, CRC Press, Boca Raton, 1995.

Paper 7/07485I; *Received* 16*th October* 1997